

## MOMENTS AND PROBABILITY DENSITY OF SATURATED INTENSITY FLUCTUATIONS IN THE TURBULENT ATMOSPHERE

**G.Ya. Patrushev**, A.P. Rostov, and O.A. Rubtsova

*Institute of Atmospheric Optics,  
Siberian Branch of the Russian Academy of Sciences  
Received October 20, 1994*

*Experimental data are analyzed on statistics of plane wave intensity fluctuations within the range of  $\beta_0$  parameter values from 6 to 18. Comparative analysis of high-order moments and histograms with theoretical models is carried out. The experimental moments exceed the available asymptotic values and become saturated within the range of  $\beta_0$  values from 7 to 18 at practically unchangeable level for the relative rms values of  $\beta$  fluctuations about 1.16–1.17. The histograms of instantaneous values of the intensity are well approximated by K-distribution. Based on the experimental data the mean number of channels,  $N$ , for multi-beam propagation through the turbulent atmosphere, is related to the value of  $\beta_0$  parameter:  $N = 6$  or  $7$  for  $\beta_0 = 7$  to  $18$ .*

During more than twenty years different authors are investigating the probability density of the intensity fluctuations of optical radiation propagating through the turbulent atmosphere. However, up to now no functional form of the probability density for extremely saturated intensity fluctuations has been established reliably. Several heuristic models were proposed, their brief analysis and comparison with the experimental data which sum up the preceding investigations were carried out in Ref. 1.

It should be noted that the proposed models were tested over an essentially limited range of turbulent conditions of propagation (the parameter  $\beta_0 = 1.21C_n^2 k^{7/6} L^{11/6}$ , where  $C_n^2$  is the structural constant of the refractive index field;  $k = 2\pi/\lambda$  is the wave number;  $L$  is the propagation path length). At the same time practically all theoretical investigations were devoted to an asymptotic analysis of the high-order moments of the intensity fluctuations.<sup>2–4</sup> Results of these investigations, strictly speaking, are valid for  $\beta_0 \gg 1$ , whereas the experimental values of  $\beta_0$  did not exceed 7 with the rare exception. Moreover, a comparison with the experimental data in most cases was insufficiently correct, since shifts and variance of the experimental moments due to limited range of received signals were not considered.<sup>1</sup>

We have measured the high-order normalized moments and histograms of the plane wave intensity fluctuations for values of  $\beta_0$  parameter significantly exceeding those in earlier measurements in order to test available theoretical dependences of the high-order moments and several models of the probability density of the intensity fluctuations.

The measurements were carried out using a well developed technique (see Ref. 1 and references therein). A V-shaped path with a reflect of the total length  $L = 3.7$  km was arranged. A high-quality mirror disk 500 mm in diameter served as a reflector; a distance between the

optical axes of direct and reflected beams in the reception place was more than 1 m that allowed the effect of intensity fluctuations enhancement due to reflection to be ignored.

Small bulk of experimental data was also obtained at the path of  $L = 400$  m. A quasi-plane wave was formed by a lens objective 500 mm in diameter with the effective beam output dimension of 8.5 cm by the level  $e^{-1}$ . The laser radiation ( $\lambda = 0.63 \mu\text{m}$ ) was received by three PMTs FEU-79 with the input diaphragms of  $\approx 0.3$  mm diameter. The central photomultiplier was placed at the visual center of the beam, two other PMTs were at a distance of 5 to 10 mm from it. Control of turbulent conditions in the atmosphere was performed by monitoring the intensity fluctuations at the path of length  $L_1 = 200$  m. Additional monitoring of homogeneity of the turbulence intensity along the path was done with an acoustic anemometer-thermometer<sup>5</sup> placed near the middle of the path. Signals from PMTs were recorded with a digital tape-recorder in four channels with the digitization frequency of 5 kHz in each channel during 5 min.

The use of signals recorded with the optical meter of  $C_n^2$  and the acoustic anemometer-thermometer data allowed the inner scale of the turbulence to be determined from the temporal fluctuation spectrum.<sup>6</sup> High reliability of recording and reproducibility of digital information (the loss coefficient  $\leq 10^{-7}$ ) and dynamic range (12 bits) allowed the histograms to be effectively estimated over the range of relative signal values  $0.01 \leq I/\langle I \rangle \leq 20 \div 25$ , i.e., three orders of magnitude wide. The measurements were carried out in June and July under the conditions of fine sunny weather at midday time. The parameter  $l_0$  was in the range of 3 – 4 mm during these measurements.

Figure 1 shows the scintillation index  $\beta = (\langle I^2 \rangle / \langle I \rangle^2 - 1)^{1/2}$  as a function of the parameter  $\beta_0$ .

Curve 1 presents averaged experimental data from Ref. 7 for a plane wave, curve 2 is the asymptotic obtained in Ref. 8:

$$\beta^2 = 1 + 0.85 (\beta_0^2)^{-2/5}, \tag{1}$$

curve 3 is calculated by the formula

$$\beta^2 = 1.74 - 0.092\beta_0 + 0.6 (2\pi l_0^2 / \lambda L)^{1/2}, \tag{2}$$

obtained in Ref. 9 for a plane wave in the region of fluctuation focus allowing for the inner scale of turbulence  $l_0 = 4$  mm. Curve 4 is the approximation of the experimental data estimated by eye.

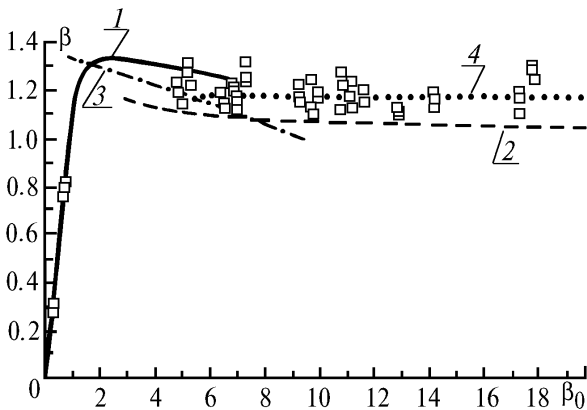


FIG. 1. The intensity fluctuation scintillation index  $\beta$  as a function of the parameter  $\beta_0$ .

As one can see from Fig. 1, in the region of weak fluctuations the experimental data agree quite well with the curve 1 and are close to it for  $\beta_0 = 6 \div 7$ , and in the saturation regime all data lie above the asymptotic curve 2 and the intensity fluctuations are saturated at the level  $\beta \approx 1.16 \div 1.17$ .

Let us consider now the high-order normalized moments  $M_n = \langle I^n \rangle / \langle I \rangle^n$  ( $n = 3, 4, 5$ ) as functions of the parameter  $\beta_0$  (Fig. 2). In the saturation region the experimental values of the high-order moments lie above the asymptotic curves (curves 1) obtained in Ref. 8:

$$M_n = n! [1 + 0.43 \frac{n(n-1)}{2} \beta_0^{-4/5}], \tag{3}$$

and asymptotes obtained by Dashen in Ref. 2 (curves 2),

$$M_n = n! \exp \left[ 0.43 \frac{n(n-1)}{2} \beta_0^{-4/5} \right], \tag{4}$$

and also exceed the level corresponding to the exponential distribution (it is shown by dashed curve in the right portion of Fig. 2).

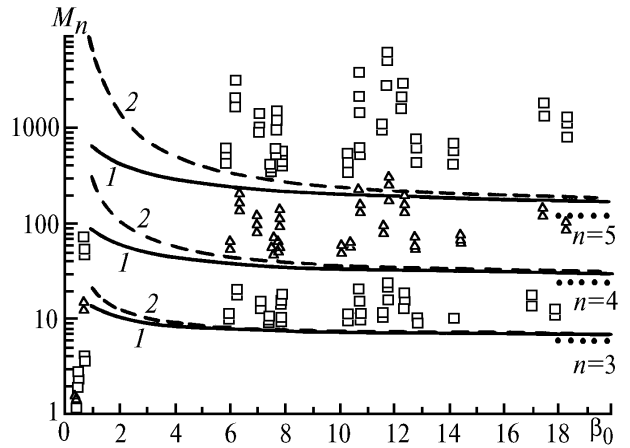


FIG. 2. The high-order normalized moments  $M_n$  ( $n = 3, 4, 5$ ) as functions of the parameter  $\beta_0$ .

Comparative analysis of the high-order moments and probability density of instantaneous values of the intensity and the model distributions gives more complete information about the character of fluctuations of the process. The high-order normalized experimental moments  $M_n$  ( $n = 3, 4, 5$ ) as functions of the second normalized moment  $M_2 = \langle I^2 \rangle / \langle I \rangle^2$  are shown in Fig. 3. Solid curves correspond to the moments of a lognormal distribution

$$P(I) = (\sqrt{2\pi}\sigma I)^{-1} \exp[-(1/2\sigma^2)(\ln I - \xi)^2];$$

$$\sigma^2 = \ln(1 + \beta^2); \quad \xi = \ln[\langle I \rangle / (1 + \beta^2)^{1/2}], \tag{5}$$

calculated taking into account the shift due to limitedness of the dynamic range under the experimental conditions ( $I_{\max} = 4095$ ;  $\langle I \rangle = 150$ ) by the formula obtained in Ref. 10. Dashed curves correspond to the moments of  $K$ -distribution:

$$\langle I \rangle P(I) = (2/\Gamma(y)) y^{(y+1)/2} I^{(y-1)/2} K_{y-1}[2(Iy)^{1/2}]; \tag{6}$$

$$y = 2 / (\beta^2 - 1); \quad y > 0,$$

where  $K_\nu(z)$  is the McDonald function. These moments are also calculated by the formula obtained in Ref. 11 taking into account the shift. As is clear from Fig. 3, the experimental moments deviate from the lognormal dependence with increasing  $M_2$  and correspond to the moments of  $K$ -distribution within the range  $2 < M_2 < 3$ ; for  $M_2 > 3$  the truncated moments of the aforesaid distributions lie so close to each other that it is difficult to reveal a correspondence of moments to any law, therefore we analyze the histograms of instantaneous values of the intensity for more detailed verification of the distribution law.

Figures 4–7 present the characteristic histograms for various values of the scintillation index  $\beta$  and parameter  $\beta_0$ . The model probability densities (5) and (6) are outlined in these figures for a comparison. Vertical bars on the plots show the rms deviation of the histogram estimation. As one can see from

Fig. 4, for weak fluctuations ( $\beta_0 < 1$ ,  $\beta < 1$ ) the experimental data are well approximated by the lognormal distribution that corresponds to the accepted model of the probability density for the weak fluctuations.<sup>7, 12</sup> As to the saturation region (Figs. 5–7), here the experimental data are close to  $K$ -distribution, but together with the data which are very well approximated by  $K$ -distribution over the whole range of the intensity values (Fig. 5), there are the histograms somewhat different from it in the deep fading region (Fig. 6). Thus, Fig. 7 presents the histograms which have very close values of  $\beta_0$  and  $\beta$  though they differ by about an order of magnitude in the fading region. Such a change in the histograms can hardly be explained within the framework of the model of stationary random process, and it is probably connected with the fact that the assumption on stationarity is valid only approximately. Nevertheless,  $K$ -distribution in the saturation regime approximates this histograms better than the lognormal and exponential ones that confirms the conclusions drawn in Ref. 13.

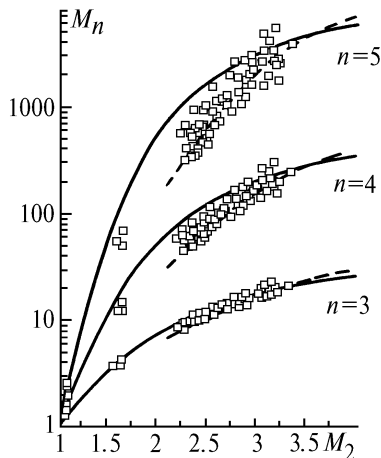


FIG. 3. The high-order normalized moments of the intensity  $M_n$  ( $n = 3, 4, 5$ ) as functions of the second normalized moment  $M_2$ .

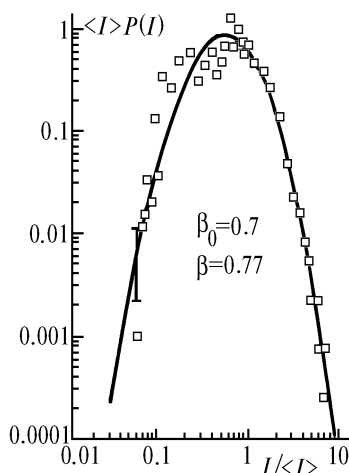


FIG. 4. Comparison of the histogram  $P(I)$  of the normalized values of the intensity  $I/\langle I \rangle$  with the lognormal distribution.

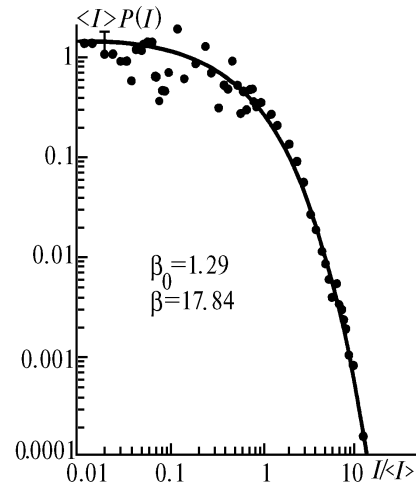


FIG. 5. Comparison of the histogram of the normalized values of the intensity with  $K$ -distribution.

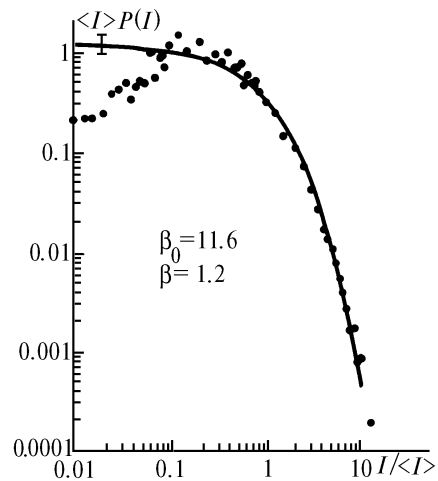


FIG. 6. Comparison of the histogram of normalized values of the intensity with  $K$ -distribution.

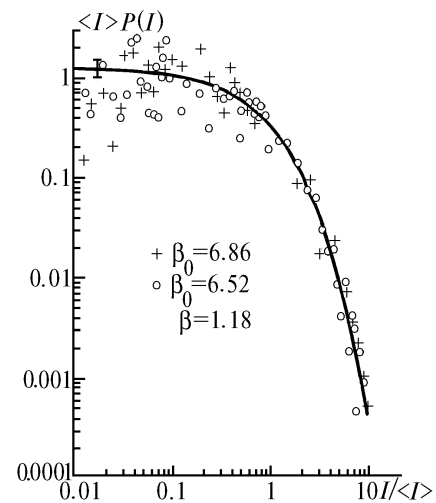


Fig. 7. Comparison of the histogram of normalized values of the intensity with  $K$ -distribution.

Let us now consider the physical scenario resulting in  $K$ -distribution. As was noted in Refs. 14 and 15, when the optical waves propagate through randomly inhomogeneous medium the refractive index fluctuations cause the appearance of a caustic peculiar points. Along every beam at a finite distance from the preceding caustic another one caustic is formed with the unit probability. The appearance of caustics results in a multi-beam regime of wave propagation. In this case not only one but several beams with different initial coordinates reach the same point. If a number of such independent channels of propagation is sufficiently large ( $\gg 12$ ) then scattered field satisfies the Gaussian statistics and, hence, the intensity probability density is exponential. In the case when the illuminated region is comparable or smaller than the spatial correlation of field fluctuations and the mean number of independent channels of propagation is small, the central limit theorem is inapplicable and the scattered field statistics differs from Gaussian form. In our case this explains why the fluctuations are saturated at the level which is greater than unity, and the probability density approaches to  $K$ -distribution curve.

Evolution of the experimental histograms from  $K$ -distribution to exponential one with increasing number of scatterers in the illuminated region is well seen from data presented in Ref. 16 where the case of the laser radiation scattering by a rough surface is considered. When the number of scatterers reaches  $\sim 50$  the probability density is close to an exponential function, and when the number of scatterers is small ( $\sim 7$ ) the obtained histograms become closer to  $K$ -distribution.

It is difficult to make based on the publications available<sup>15,16</sup> more correct estimation of the mean number of the propagation channels and their variance in the region of saturated fluctuations.

The observed spread in values of the histograms in the region of deep fading is most likely connected with the variation of the number of scattering channels, whose rms number is comparable with the mean value.

The above discussed circumstances also explain the fact that statistics observed in the experiments on a spherical wave reflection from an array of corner-cube reflectors differ from Gaussian law.<sup>17</sup> In spite of the fact that a number of corner reflectors in the experiment is rather large (twelve), at a distance of the order of the array size the field fluctuation correlation takes place and therefore the mean number of independent propagation channels contributing to the receiving field is smaller than the number of reflectors. Having spaced the array elements at a distance exceeding the correlation radius of the wave field so that the beams arrived from individual corners can be considered independent, we may try to obtain the exponential distribution in the experiment.

Thus, it is shown in the paper that our experimental data on the intensity fluctuation moments in the saturation regime ( $\beta_0 \approx 6-19$ ) lie above all the calculated asymptotic curves, and saturation occurs at the stable level of  $\beta=1.16-1.17$  which exceeds the level corresponding to the exponential distribution. It is also shown that starting from the values of the parameter  $\beta_0 \gtrsim 6-18$   $K$ -distribution approximates the experimental data quite well. In this case a number of the channels for multi-beam propagation is 6 or 7.

#### ACKNOWLEDGMENT

This work was supported in part by Russian Fundamental Research Foundation Grant No. 94-02-03734-a.

#### REFERENCES

1. G.Ya. Patrushev and O.A. Rubtsova, Atmos. Oceanic Opt. **6**, No. 11, 760-769 (1993).
2. R. Dashen, Opt. Letters. **10**, No. 4, 110 (1984).
3. Q.-Y. Wang and R. Dashen, J. Opt. Soc. Am. **10**, No. 6, 1226 (1993).
4. R. Dashen, et. al., J. Opt. Soc. Am. **10**, No. 6, 1233 (1993).
5. G.Ya. Patrushev, A.P. Rostov, and A.P. Ivanov, Atmos. Oceanic Opt. **7**, No. 11-12, 890-891 (1994).
6. E.A. Monastyrnyi, G.Ya. Patrushev, A.I. Petrov, and V.V. Pokasov, "Technique for obtaining the inner scale of turbulence and equipment for its realization," Invention Certificate No. T 913794.
7. A.S. Gurvich, A.I. Kon, V.L. Mironov, and S.S. Khmelevtsov, *Laser Radiation in the Turbulent Atmosphere* (Nauka, Moscow, 1976), 280 pp.
8. K.S. Gochelashvili and V.I. Shishov, Zh. Eksp. Teor. Fiz. **66**, 1237 (1974).
9. S.M. Flatte, Q.Y. Wang, and I. Martin, J. Opt. Soc. Am. **10**, No. 11, 2354 (1993).
10. G.Ya. Patrushev, T.P. Pecherkina, and A.P. Rostov, Avtometriya, No. 3, 22 (1985).
11. A. Consortini and R. Hill, Opt. Lett. **12**, No. 5, 304 (1987).
12. V.I. Tatarskii, *Wave Propagation in a Turbulent Medium* (Dover, New York, 1968).
13. G.Ya. Patrushev and O.A. Rubtsova, Atmos. Oceanic Opt. **5**, No. 7, 453-455 (1992).
14. Yu.A. Kravtsov, Zh. Eksp. Teor. Fiz. **55**, No. 3, 798 (1968).
15. E.Z. Gribova and A.I. Saichev, Radiotekhn. Elektron. **39**, No. 2, 193 (1994).
16. I.A. Popov, N.V. Sidorovsky, and L.M. Veselov, Opt. Commun. **97**, No. 5-6, 304 (1993).
17. G.Ya. Patrushev, A.I. Petrov, and O.A. Rubtsova, Atm. Opt. **2**, No. 3, 216-226 (1989).